PCCP

Dynamic Article Links

Cite this: *Phys. Chem. Chem. Phys.*, 2012, **14**, 6509–6513

www.rsc.org/pccp

PAPER

Solubility of gold nanoparticles as a function of ligand shell and alkane solvent

Brandon C. Lohman, Jeffrey A. Powell, Sreeram Cingarapu, Christer B. Aakeroy, Amit Chakrabarti, Kenneth J. Klabunde, Bruce M. Law and Christopher M. Sorensen*

Received 29th February 2012, Accepted 8th March 2012
DOI: 10.1039/c2cp40645d

The solubility of *ca.* 5.0 nm gold nanoparticles was studied systematically as a function of ligand shell and solvent. The ligands were octane-, decane-, dodecane- and hexadecanethiols; the solvents were the n-alkanes from hexane to hexadecane and toluene. Supernatant concentrations in equilibrium with precipitated superclusters of nanoparticles were measured at room temperature (23 °C) with UV-Vis spectrophotometry. The solubility of nanoparticles ligated with decane- and dodecanethiol was greatest in n-decane and n-dodecane, respectively. In contrast, the solubility of nanoparticles ligated with octane- and hexadecanethiol showed decreasing solubility with increasing solvent chain length. In addition the solubility of the octanethiol ligated system showed a nonmonotonic solvent carbon number functionality with even numbered solvents being better solvents than neighboring odd numbered solvents.

I. Introduction

Modern synthetic chemistry has produced a wide variety of nanoparticles (NPs) with a high degree of both chemical and physical uniformity.[1–3] These NPs can be surface ligated with a range of organic compounds yielding NP colloids that are stable against irreversible aggregation. When a surface ligated NP colloid is destabilized, typically by evaporating or changing the solvent, a precipitate forms which is usually a three dimensional superlattice due to the NP size uniformity.[4] Moreover, there is qualitative evidence that these colloids can act as solutions with characteristic temperature dependent solubility[5,6] and nucleation phenomena.[7] Thus, a suspension of NP monomers can be in equilibrium with precipitated superclusters of NPs and in that manner the suspension is a solution as well (NPs are often referred to as ''clusters'' so we use the term ''supercluster'' to mean a cluster of clusters).

The analogy that NP suspensions are like molecular solutions with the NPs acting like large molecules is very attractive since it would allow us to use much of what we know about molecular solutions to handle and assemble NPs. However, NPs are far more mutable than most molecules, and much of their mutability lies in their ligand shells. Moreover, it is reasonable to expect that NP solubility will be greatly affected by the ligand shell. These ligand shells have been shown to be capable of harboring small amounts of alkylammonium surfactants that can modify the NP solubility.[8,9] The shape of the ligand shells depends strongly on the size of the underlying core, the chain length and environment, the solvent, and the chain terminal groups.[10,11] Moreover the ligands can be highly mobile on and in the NP and can lower the core melting temperature.[12] Recent work[13,14] has shown that NP solubility can have complex dependencies on the capping ligand and solvent for NPs with mixed hydrophilic and hydrophobic ligands. Thus it appears that systematic studies of the effects of ligand and solvent on NP solubility are warranted.

In an effort to gain more understanding of the behaviour of NP solutions in general and some details regarding the effects of ligands and solvents on these solutions, this paper presents the solubility behaviours of gold NPs as a function of both the capping ligand and the solvent. The work is confined to room temperature and a simple series of alkyl thiol ligands and n-alkyl solvents. Despite this simplicity a variety of interesting and unexpected trends are uncovered.

II. Experimental methods

To synthesize our particles we used the inverse micelle method followed by digestive ripening[15] as described by Prasad *et al.*[16] Briefly, 34 mg of gold(III) chloride was dissolved into 10 mL of a toluene solution 0.02 M dodecyldimethylammonium bromide (DDAB). 36 μL of an aqueous solution of 9.4 M sodium borohydride ($NaBH_4$) was added dropwise to reduce the gold to elemental form providing a colloid composed of polydispersely sized particles. An n-alkanethiol, either octane-, decane-, dodecane- or hexadecanethiol, capping ligand was

Department of Physics and Chemistry, Kansas State University, Manhattan, KS 66506-2601, USA. E-mail: sor@phys.ksu.edu; Fax: 785-532-6806; Tel: 785-532-1626

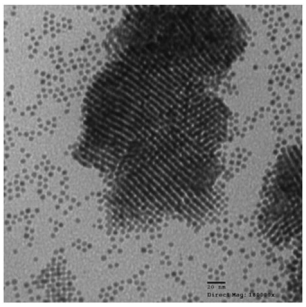

Fig. 1 TEM image of gold nanoparticle monomers and a few superclusters. The ligand was dodecanethiol.

added in the amount of a molar ratio of 30 : 1 ligand:Au to this "as prepared" system to displace the surfactant and stabilize the gold particles against agglomeration. The gold particles were precipitated and excess ligand, surfactant, and reducing agent were removed by washing with ethanol. The precipitated particles were re-dispersed in 10 mL of toluene in the presence of the same 30 : 1 excess n-alkanethiol ligand and heated under reflux (digestively ripened) for a set time, typically one hour. The digestive ripening equilibrates the size distribution to yield a quasi-monodisperse system. The NP "monomers," that is, individual crystals of gold surrounded by the alkanethiol ligand, were about 5 nm in diameter with a 10% standard deviation. Different ligands yield different diameters of 4.5, 4.7, 4.7 and 5.5 nm for the C8, C10, C12 and C16 ligands, respectively.[6] An example Transmission Electron Microscope (TEM) picture of these NPs is shown in Fig. 1.

In preparation for solubility studies, the digestively ripened NPs were held in solution with toluene. They were then precipitated with ethanol and the supernatant containing the toluene solvent and excess ligand was discarded. Then the precipitated NPs were subjected to vacuum-drying. The ethanol precipitation was straightforward for NPs ligated with octanethiol, decanethiol and dodecanethiol, but hexadecanethiol posed unique difficulties. Hexadecanethiol's freezing point of 18 °C is above those of the other thiols and near room temperature. For this reason crystals of solid hexadecanethiol were sometimes present in the supernatant when the NP solution was precipitated with ethanol. The hexadecanethiol crystals were difficult to completely remove from the nanoparticles, and our vacuum-dried hexadecanethiol ligated NPs were quite "wet" with leftover excess ligand at worst to slightly pasty at best. To remove excess hexadecanethiol ligand we precipitated with "warm ethanol" at 30–35 °C and centrifuged at 300 g for five minutes. The still-warm supernatant containing excess ligand was discarded and the pellets were redissolved with a drop of toluene, collected and vacuum-dried for over 6 h.

Once the NPs were in a dried state, masses great enough to yield saturated solutions (about 2 mg) were dissolved in 1000 μL (typically) of various n-alkane solvents between n-hexane and n-hexadecane and the aromatic solvent, toluene. This dissolution and all subsequent experiments were performed at ambient room temperature of 23 ± 1 °C. These "stock solutions," were sonicated to aid dissolution and left to settle to ensure saturation of monomers in equilibrium with a precipitate of superclusters. We refer to all stock solutions derived from a single lot of dried NPs with a given ligand as a "sample series." For our experiments, excess ligand in a ratio of 5% by volume of solvent was added to the stock solutions.

The saturation concentration of NP monomers dissolved in the supernatant in equilibrium with precipitated superclusters of NPs was measured by UV-Vis spectroscopy. To do this ~100 μL aliquots of each solution in a sample series were centrifuged under 12 000 g acceleration for approximately 10 to 15 min. The hydrodynamic diameter of the NPs including the ligand shell is 8 nm, whereas the superclusters are 200 nm or greater.[7] Using the Stokes drag formula one can show that this would cause the single NPs of the supernatant to only fall about 0.1 mm, while the superclusters would fall about 6 cm, greater than the 2 cm centrifuge tube. Visual inspection showed that this method was very effective in separating the precipitate from the NP supernatant, consistent with the Stokes calculation, leaving a supernatant of monomers in equilibrium with the precipitate. Most importantly, conclusive evidence that only monomers exist in the supernatant is shown by the UV-Vis spectra of the supernatants which showed only the transverse plasmon mode peaking at 530 nm.[17] The spectrum of a dimer has a longitudinal mode as well at 600 nm[17,18] which shows as a readily apparent shoulder on the transverse mode. Larger aggregates continue the enhancement of this red shifted shoulder.[18] No shoulders were seen in the spectra of our supernatants after the centrifuge step and the shape of the plasmon at 530 nm was compared to those in dilute non-precipitated systems and found to be identical.

Since the ligand shell is important for the NP solubility, we now discuss the nature of the shell. Surface studies[19]of self assembled monolayers of alkane thiols indicate each thiol occupies an area of 0.224 nm^2. For a 5 nm gold NP this implies a molar ratio of gold to alkane thiol of *ca.* 8. We have evidence that the alkane thiols form a thiolate on the NP surface and we have measure evolution of hydrogen gas with a gold to H atom ratio of *ca.* 8.[20] This implies that the alkane thiols are packed as tight as they can be on the NP surface. Another important observation is that the superlattices of our systems all show interparticle spacing consistent with alkane inter digitization. This observation also implies a uniform and complete ligand coating.

All the data shown below are the result of at least two independent measurements. In some cases a slow drift with time for the solubility was observed with the NPs becoming less soluble at a rate of about 10% per week. Exposure of the samples to light and oxygen increases their instability with time, but the drift persisted for dark, carefully contained samples. This drift did not significantly affect the functionalities of the solubility. The error bars provided in the result graphs below are from the highest to lowest measured concentration in a given ensemble of measurements (run-to-run variation) for a given system.

Some of the samples showed idiosyncrasies. For example, dodecanethiol ligated NP solutions required centrifuge treatment for 60 min because short-chain solvent solutions (hexane and heptane) did not "pellet out" after 15 min. A hard nugget of clusters did appear at the bottom of the centrifugation vials, but a turbid layer appeared between the solid pellet of clusters and the transparent supernatant of monomers. A full hour of

centrifugation was needed to push the interface between the turbid phase and the supernatant phase to the bottom of the vial. Given this, the solvent hexane was problematic because it evaporated quickly making the concentration measurement difficult. Consequently, data were not obtained for NPs ligated with dodecanethiol in hexane.[21]

For all samples *ca.* 25–50 μL of the supernatant was pipetted into a clean quartz cuvette of 1 mm path length and 100 μL nominal volume, and absorbance data were taken by a Cary Win-UV UV-Vis Spectrophotometer. The UV-Vis apparatus was normalized by taking baseline absorbance measurements on a blank sample of either n-hexane or ethanol which are both colorless and transparent in the visible range. Absorbance data were converted into concentration of gold in the supernatant in equilibrium with the precipitate (measured in moles of gold NPs per liter) with a previously determined calibration.[22] Typically three data points were collected for each solvent/NP combination. All measurements were made at room temperature.

The term "solubility" implies a history independent equilibrium between single solid and dissolved phases. History independence in our work is supported by the reproducibility of our measurements despite different synthetic batches, ratios of dried nanoparticle powders to solvent, sonication times, and plateaus with centrifuging times. The fact that UV-Vis spectra of the supernatant shows only the surface plasmon of the single nanoparticle strongly supports the contention that the dissolved phase is indeed a single phase of individual gold nanoparticles. The nature of the solid precipitate is not known directly; it could be a superlattice of close packed spheres or an amorphous aggregate. However, it is very likely a superlattice as observed numerous times with *ex situ* TEM photographs such as Fig. 1. Moreover, Compton and Osterloh[23] collected clusters of nanoparticles that settled from nucleated solutions and found them to be superlattice crystals.

III. Results and analysis

1. Gold nanoparticles with octanethiol ligands

Fig. 2 shows the equilibrium saturation concentration of gold NPs ligated with octanethiol in a variety of hydrocarbon solvents at room temperature. Note that we use concentration units as nanomoles of NPs per liter of solution; a conversion is that 1000 nM NP concentration corresponds to 0.78 mg/mL of gold for a 5.0 nm NP. Fig. 2 displays an interesting even/odd effect in the saturation concentrations depending on the number of carbon atoms in the alkane solvent chains, with even numbered solvents having relatively higher solubilities than odd. The maximum solubility appears to be when the NPs are dissolved in n-hexane with an overall decreasing solubility with longer chains. The absolute concentrations are noticeably lower than the NPs with other ligands studied, see below.

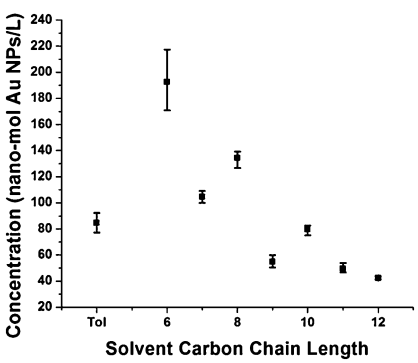

Fig. 2 Equilibrium saturation concentration *vs.* solvent for octanethiol ligated gold nanoparticles in n-alkanes (chain length 6 through 12) and toluene (Tol).

2. Gold nanoparticles with decanethiol ligands

Fig. 3 shows the equilibrium saturation concentration of gold NPs ligated with decanethiol in a variety of hydrocarbon solvents at room temperature. The data show a fairly smooth trend with a maximum saturation concentration corresponding to n-decane as a solvent, with a minor, reproducible "hiccup" near n-nonane. Ignoring this anomaly for the moment, the general trend peaks with the solvent having the same carbon number as the ligand. This implies a "like dissolves like" explanation, although the "likeness" is quite tenuous, since only the ligand has a similarity to the solvent. The reproducible anomaly at nonane, on the other hand, is reminiscent of the even/odd behaviour seen for the octanethiol ligated particles above.

3. Gold nanoparticles with dodecanethiol ligands

Fig. 4 shows the equilibrium saturation concentration of gold NPs ligated with dodecanethiol in a variety of hydrocarbon solvents at room temperature. The solubility trend for the alkane solvents shows a peak at undecane, which has nearly the same carbon atom number as the ligand to suggest again a "like dissolves like" description.

4. Gold nanoparticles with hexadecanethiol ligands

Fig. 5 shows the equilibrium saturation concentration of gold NPs ligated with hexadecanethiol in a variety of hydrocarbon solvents at room temperature. The data show a decreasing solubility with increasing chain length for n-alkane solvents. This and the relatively low solubility are similar to the octanethiol ligated nanoparticles but without the even/odd behaviour.

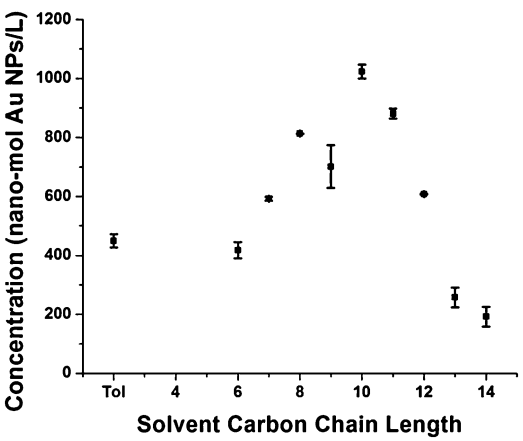

Fig. 3 Equilibrium saturation concentration *vs.* solvent for decanethiol ligated nanoparticles in n-alkanes (chain length 6 through 14) and toluene (Tol).

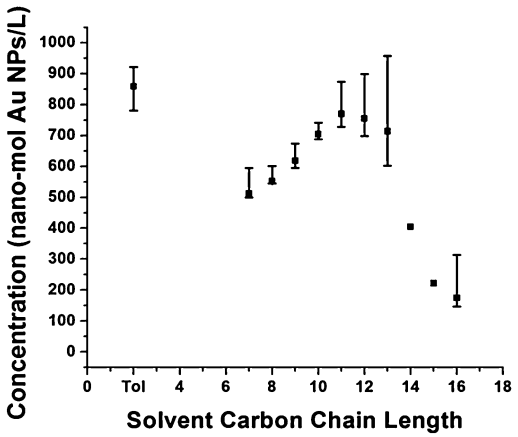

Fig. 4 Equilibrium saturation concentration *vs.* solvent for dodecanethiol ligated nanoparticles in n-alkanes (chain length 7 through 16) and toluene (Tol). For dodecanethiol ligated NPs dissolved in tetradecane and pentadecane, only one data point was acquired. As a consequence, no error bars are provided for these points.

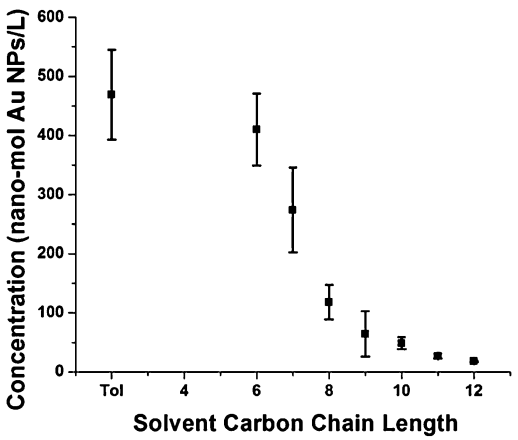

Fig. 5 Equilibrium saturation concentration *vs.* solvent for hexadecanethiol-ligated nanoparticles in n-alkanes (chain length 6 through 12) and toluene (Tol).

IV. Discussion

The data from all four NP systems are plotted together in Fig. 6. The systems appear to differentiate into two classes:

(1) Two systems with a peak in the solubility when the carbon chain length of the alkane solvent is the same as the alkanethiol ligand to imply the tenuous "like dissolves like" behaviour. This holds for the medium-length ligands, decanethiol and dodecanethiol.

(2) Two systems with a general trend of decreasing solubility with increasing solvent molecule chain length valid for the shortest and longest ligands, octanethiol and hexadecanethiol.

Superimposed somewhat on these two groups is the zigzag, even/odd functionality (greater solubility for even numbered solvents) with solvent chain length seen in the NPs ligated with octanethiol and one instance with the decanethiol ligation. The peak in solubility for the first class leads to significantly larger solubility for the NPs ligated with these ligands in the longer chain solvents. On the other hand, the solubilities for all the NPs appear to be converging to a rough equality as the solvent chain shortens.

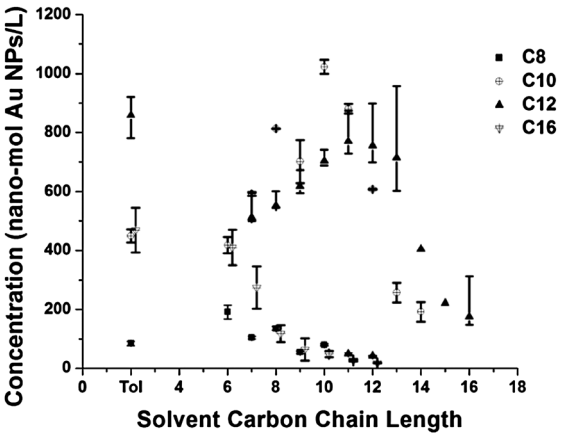

Fig. 6 Equilibrium saturation concentration *vs.* solvent for all four nanoparticle systems.

We have recently developed a phenomenological model for the effective interaction potential between two ligated gold nanoparticles.[24] In our phenomenological model, the ligands are viewed as flexible chains with free-energy of mixing and elastic contributions, due to ligand compressions, in addition to van der Waals interactions between the metallic cores. This model is successful in calculating the interparticle distances in superlattices and the increasing solubility trend for NPs dissolved in toluene.

Encouraged by the success of this recent work, we continue to model the ligand chains as flexible polymers and consider the free energy of mixing in terms of the Flory χ-parameter between[25,26] the solvent and the *flexible* tethered chains for the current work. The Flory χ-parameter has two sets of contributions, enthalpic and entropic in origin. The enthalpic part is computed in terms of the Scatchard and Hildebrand theory[27] as $(V_m/RT)(\delta_s-\delta_m)^2$ where R is the gas constant, T the temperature, V_m is the molar volume of the solvent and $\delta_{solvent}$ and δ_{solute} are Scatchard and Hildebrand solubility parameters. The entropic part is taken to be a constant equal to 0.34. Thus,

$$\chi = (V_m/RT)(\delta_{solvent}-\delta_{solute})^2 + 0.34 \qquad (1)$$

in our model calculations.

Within the range of the Flory theory, $\chi > 1/2$ corresponds to poor-solvent region and $\chi < 1/2$ conforms to good solvent region. Thus in order to compare with experimental measurements of solubility, we consider $\chi - 1/2$ as a gauge of the solvent's effectiveness. Values for the Scatchard and Hildebrand solubility parameters where obtained from the literature.[28] Unfortunately, we could not find solubility parameter data for n-tetradecane and n-pentadecane.

This procedure was somewhat effective for dodecanethiol ligated particles if we substituted $\delta_{solute} = \delta_{ligand}$. The results are shown in Fig. 7 which replicates the data of Fig. 4 and adds the $\frac{1}{2} - X$ parameter on the right-hand axis. This axis has been scaled by a multiplicative factor to yield the closest fit to the data. The fit is pretty good except for the hexadecane solvent. Furthermore, the value of $\frac{1}{2} - X$ is negative for toluene, yet experiment shows that toluene is a good solvent. The good solubility in toluene could be due to traces of the DDAB

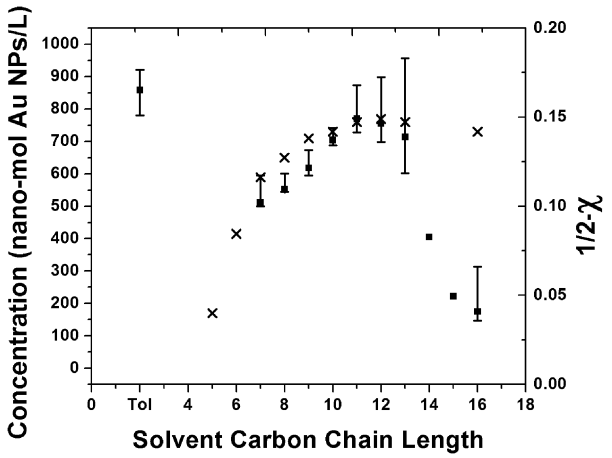

Fig. 7 Equilibrium saturation concentration *vs.* solvent for dodecanethiol ligated nanoparticles in n-alkanes (chain length 7 through 16) and toluene (Tol). Flory parameters, right hand axis are plotted with X symbols.

surfactant as implied by Waters *et al.*[8] We expect that the NP solubility parameter is very likely affected by more than the composition of its ligand shell; thus the semiquantitative fit in Fig. 7 is remarkable. Other factors that might affect solubility include the NP core and the conformational aspects of the ligand shell, as discussed briefly in the introduction, which could well be causing the behaviours seen for the other ligand shells.

V. Conclusions

These results are indeed perplexing. The simple empirical rule of "like dissolves like" gives some solace but only for the ligands of intermediate length, C10 and C12, and yet is troubling because it ignores so much. Remarkably, the two extremes of ligand length, C8 and C16, are similar to each other and stand apart from the intermediate length ligands. This seems to void any argument invoking relative ligand chain flexibility/stiffness. It also appears to void those that would invoke the concept that shorter ligands allow the gold NP cores to approach more closely and thus lower the solubility *via* stronger van der Waals attraction.

Alkane chain carbon number even/odd behaviours are well known in the physical properties of alkanes and alkane derivatives.[29] However, we know of no such behaviour with regard to solvent ability.

Given our results here and the complexity of similar previous results,[13,14] it is apparent that extensive and systematic experiments on nanoparticle solubility could uncover a great variety of interesting phenomena.

Acknowledgements

We thank Professor John Tomich for use of some of his laboratory equipment. We thank Evan Hurley for help with the synthesis of some of the particles. This work was supported by NSF NIRT Grant CTS0609318.

References

1 *Nanoscale Materials in Chemistry*, ed. K. J. Klabunde, Wiley Interscience, New York, NY, 2001.
2 M.-C. Daniel and D. Astruc, *Chem. Rev.*, 2004, **104**, 293.
3 J. P. Wilcoxon and B. L. Abrams, *Chem. Soc. Rev.*, 2006, **35**, 1162.
4 B. L. V. Prasad, C. M. Sorensen and K. J. Klabunde, *Chem. Soc. Rev.*, 2008, **37**, 1871–1883.
5 X. M. Lin, G. M. Wang, C. M. Sorensen and K. J. Klabunde, *J. Phys. Chem. B*, 1999, **103**, 5488.
6 B. L. V. Prasad, S. I. Stoeva, C. M. Sorensen and K. J. Klabunde, *Langmuir*, 2002, **18**, 7515.
7 H. Yan, S. Cingarapu, K. J. Klabunde, A. Chakrabarti and C. M. Sorensen, *Phys. Rev. Lett.*, 2009, **102**, 095501.
8 C. A. Waters, A. J. Mills, K. A. Johnson and D. J. Schriffin, *Chem. Commun.*, 2003, 540–541.
9 M. N. Martin, J. I. Basham, P. Chando and S.-K. Eah, *Langmuir*, 2010, **26**, 7410–7417.
10 C. Singh, P. K. Ghorai, M. A. Horsh, A. M. Jackson, R. G. Larson, F. Stellacci and S. C. Glotzer, *Phys. Rev. Lett.*, 2007, **99**, 226106.
11 J. M. D. Lane and G. S. Grest, *Phys. Rev. Lett.*, 2010, **104**, 235501.
12 B. J. Henz, T. Hawa and M. R. Zachariah, *Langmuir*, 2008, **24**, 773–783.
13 A. Centrone, E. Penzo, M. Sharma, J. W. Myerson, A. M. Jackson, N. Marzari and F. Stellacci, *Proc. Natl. Acad. Sci. U. S. A.*, 1998, **105**, 9886–9891.
14 O. Uzun, Y. Hu, A. Verma, S. Chen, A. Centrone and F. Stellacci, *Chem. Commun.*, 2008, 196.
15 X. M. Lin, C. M. Sorensen and K. J. Klabunde, *J. Nanopart. Res.*, 2000, **2**, 157.
16 B. L. V. Prasad, S. I. Stoeva, C. M. Sorensen and K. J. Klabunde, "Digestive Ripening Agents for Gold Nanoparticles: Alternatives to Thiols", *Chem. Mater.*, 2003, **15**, 935–942.
17 S. Link, M. B. Mohamed and M. A. El-Sayed, *J. Phys. Chem. B*, 1999, **103**, 3073–3077.
18 G. Chen, Y. Wang, L. H. Tan, M. Yang, L. S. Tan, Y. Chen and H. Chen, *J. Am. Chem. Soc.*, 2009, **131**, 4218–4219.
19 G. E. Poirier and E. D. Pylant, *Science*, 1996, **272**, 1145–1148.
20 C. Parsons, D. Jose, C. M. Sorensen and K. J. Klabunde, *J. Phys. Chem.* under review.
21 B. Lohman and *MS Thesis*, Kansas State University, 2009, unpublished.
22 H. Yan, *PhD Thesis*, Kansas State University, 2009, unpublished, http://hdl.handle.net/2097/2336.
23 O. C. Compton and F. E. Osterloh, *J. Am. Chem. Soc.*, 2007, **129**, 7793.
24 S. J. Khan, F. Pierce, C. M. Sorensen and A. Chakrabarti, *Langmuir*, 2009, **25**, 13861.
25 P. J. Flory, *Discuss. Faraday Soc.*, 1970, **49**, 7.
26 *Polymer Science and Technology*, ed. J. F. Fried, Prentice Hall, Upper Saddle River, NJ, 2003.
27 *Molecular Theory of Fluid-Phase Equilibria*, ed. J. M. Prausnitz, R. N. Lichtenthaler and E. Gomez de Azevedo, Prentice Hall, Englewood Cliffs, NJ, 1986.
28 *Physical and Thermodynamic Properties of Pure Chemicals Data Compilation*, ed. T. E. Daubert, R. P. Danner, H. M. Sibul and C. C. Sebins, Taylor and Francis, Bristol, PA, 1997.
29 H. D. Burrows, *J. Chem. Educ.*, 1992, **69**, 69.